

Does disc fragmentation prevent the formation of supermassive stars in protogalaxies?

Kohei Inayoshi¹ ^{*} and Zoltán Haiman¹

¹*Department of Astronomy, Columbia University, 550 West 120th Street, New York, NY 10027, USA*

23 September 2014

ABSTRACT

Supermassive stars (SMSs; $\gtrsim 10^5 M_{\odot}$) formed in the first protogalaxies with virial temperature $T_{\text{vir}} \gtrsim 10^4$ K are expected to collapse into seeds of supermassive black hole in the high-redshift Universe ($z \gtrsim 7$). Fragmentation of the primordial gas is, however, a possible obstacle to SMS formation. We discuss the expected properties of a compact, metal-free, marginally unstable nuclear protogalactic disc, and the fate of the clumps formed in the disc by gravitational instability. Interior to a characteristic radius $R_f = \text{few} \times 10^{-2}$ pc, the disc fragments into massive clumps with $M_c \sim 30 M_{\odot}$. The clumps grow via accretion and migrate inward rapidly on a time-scale of $\sim 10^4$ yr, which is comparable or shorter than the Kelvin-Helmholtz time $> 10^4$ yr. Some clumps may evolve to zero-age main-sequence stars and halt gas accretion by radiative feedback, but most of the clumps can migrate inward and merge with the central protostar before forming massive stars. Moreover, we found that dust-induced fragmentation in metal-enriched gas does not modify these conclusions unless $Z \gtrsim 3 \times 10^{-4} Z_{\odot}$, because clump migration below this metallicity remains as rapid as in the primordial case. Our results suggest that fragmentation of a compact, metal-poor disc can not prevent the formation of an SMS.

Key words: quasars: general — cosmology: theory — dark ages, reionization, first stars.

1 INTRODUCTION

Observations of high-redshift quasars reveal that supermassive black holes (SMBHs) with mass of $\gtrsim 10^9 M_{\odot}$ already exist as early as redshifts $z \gtrsim 6$ (Fan 2006; Willott et al. 2007; Mortlock et al. 2011). Gas accretion and mergers of the remnant black holes (BHs) formed by the collapse of first-generation stars ($\sim 100 M_{\odot}$) have been considered for producing such SMBHs (e.g. Haiman & Loeb 2001; Volonteri et al. 2003; Li et al. 2007). However, various forms of radiative feedback can prevent efficient BH growth, making it difficult to reach $\gtrsim 10^9 M_{\odot}$ within the age of the high-redshift Universe (Johnson & Bromm 2007; Alvarez et al. 2009; Milosavljević et al. 2009; Park & Ricotti 2012; Tanaka et al. 2012).

One possible alternative solution is the rapid formation of supermassive stars (SMSs; $\gtrsim 10^5 M_{\odot}$) and their subsequent collapse directly to massive BHs in the first galaxies (e.g., Loeb & Rasio 1994; Begelman et al. 2006; Lodato & Natarajan 2006). The massive seed BHs, formed by direct collapse, shorten the total SMBH growth time suf-

ficiently, even in the presence of subsequent radiative feedback (e.g. Tanaka & Haiman 2009; Di Matteo et al. 2012).

SMSs can form out of primordial gas in massive ‘atomic cooling’ haloes with virial temperatures $T_{\text{vir}} \gtrsim 10^4$ K, if H_2 formation and line cooling are prohibited through the pre-stellar collapse. Possible mechanisms to suppress H_2 formation are photo dissociation by far-ultraviolet (FUV) radiation (Omukai 2001; Bromm & Loeb 2003; Dijkstra et al. 2008; Regan & Haehnelt 2009; Shang et al. 2010; Inayoshi & Omukai 2011; Wolcott-Green et al. 2011; Johnson et al. 2013) and collisional dissociation (Inayoshi & Omukai 2012; Fernandez et al. 2014). In the absence of H_2 , the primordial gas remains warm ($\sim 8,000$ K) and may collapse monolithically without strong fragmentation (Bromm & Loeb 2003; Shang et al. 2010; Latif et al. 2013; Inayoshi et al. 2014). The resulting central protostar can grow via accretion at a high rate of $\gtrsim 0.1 M_{\odot} \text{ yr}^{-1}$. If the accretion rate maintains such a high value, the embryonic protostar evolves to a SMS with mass of $\gtrsim 10^5 M_{\odot}$. The SMS collapses as a whole to a single BH either directly (Shibata & Shapiro 2002), or via the intermediate stage of a close binary BH (Reisswig et al. 2013), through a general relativistic instability (e.g., Zeldovich & Novikov 1971; Shapiro & Teukolsky 1983). The massive remnant

* E-mail: inayoshi@astro.columbia.edu

BH is then a promising seed that can grow into one of the observed SMBHs at $z \approx 6 - 7$.

In the scenario above, a major unresolved question is whether rapid accretion will continue unabated through the protostellar evolution. Recent high-resolution simulations by Regan et al. (2014) suggest that the compact nuclear accretion disc, surrounding a central embryonic protostar, is gravitationally unstable. Thus, self-gravitating clumps are expected to form during the early stages of the accretion phase. Such efficient fragmentation could prevent the rapid growth of the central protostar, and preclude eventual SMS formation. This is analogous to the fragmentation of gravitationally unstable discs in the cores of lower mass ‘minihaloes’, which had been suggested to reduce the characteristic masses of Population III (Pop III) stars (Stacy et al. 2010; Greif et al. 2011). Moreover, if the gas is slightly polluted by heavy elements ($Z \lesssim 10^{-4} Z_{\odot}$), dust cooling can decrease the temperature and induce the fragmentation (Omukai et al. 2008), which would be a further obstacle to SMS formation. Because of this, the existence of the pristine, metal-free gas has often been considered as a necessary condition of forming a SMS in semi-analytical models (e.g., Agarwal et al. 2012; Dijkstra et al. 2014). We note that even very efficient fragmentation may not prevent accretion on to a central point source (e.g., Escala 2007) and the rapid inward migration of the fragments, on a time-scale comparable to the orbital period, may help its growth further (e.g., Ceverino et al. 2010). In our context, however, even a slow down of the accretion rate could bring it below the critical value required for SMS formation.

In this paper, motivated by the above, we discuss the expected properties of a compact, marginally unstable nuclear protogalactic disc, and the fate of the clumps formed in the disc by gravitational instability. Using analytical models, we argue that despite fragmentation, the growth of a SMS remains the most likely outcome. The reason for this conclusion is the rapid inward migration of the fragments, and their merger with the central protostar.

The rest of this paper is organized as follows. In § 2, we describe the basic model of the fragmenting disc and of the clumps formed in the disc. In § 3, we discuss the fate of the clumps, considering various important processes: migration, accretion, contraction, and star-formation by reaching the zero-age main sequence (ZAMS). We also consider the possibility that radiative feedback from massive stars, formed from the clumps, may halt gas accretion on to the whole system. In § 4, we discuss whether metal pollution and associated dust cooling could prohibit SMS formation. Finally, we discuss our results and summarize our conclusions in § 5.

2 FRAGMENTATION OF THE ACCRETION DISC AROUND A SUPERMASSIVE STAR

2.1 Basic equations

We consider the properties of a disc formed after the collapse of primordial gas inside an atomic cooling halo, when molecular hydrogen formation is suppressed. Since the parent gas cloud is hot ($T \sim 8000$ K), the accretion rate on to

the disc is high:

$$\dot{M}_{\text{tot}} \sim \frac{c_s^3}{G} \sim 0.1 M_{\odot} \text{ yr}^{-1} \left(\frac{T}{8000 \text{ K}} \right)^{3/2}, \quad (1)$$

where c_s is the sound speed and G is the gravitational constant (Shu 1977; Stahler et al. 1986). The accretion disc around the central protostar can become unstable against self-gravity. To understand the stability of the disc, Toomre’s parameter (Toomre 1964) defined by

$$Q = \frac{c_s \Omega}{\pi G \Sigma} \quad (2)$$

is often useful, where Ω is the orbital frequency and Σ is the surface density of the disc. In the marginal case of $1 \lesssim Q \lesssim 2$, strong spiral arms are formed in the disc. The spiral arms redistribute angular momentum and heat the disc by forming shocks (e.g., Vorobyov & Basu 2005, 2006). The resulting disc is self-regulated to the marginal state. Thus, we here assume $Q \simeq 1$.

Since the gas temperature in the atomic cooling halo is kept near ~ 8000 K, the external accretion rate on to the disc, from larger radii, is also nearly constant. We estimate the surface density of the self-regulated disc by assuming that it is in steady state, and that it has an effective viscosity ν (arising from gravitational torques),

$$\Sigma = \frac{\dot{M}_{\text{tot}}}{3\pi\nu}. \quad (3)$$

The scale-height of the disc is estimated from vertical hydrostatic balance,

$$H = \frac{c_s}{\Omega}. \quad (4)$$

We define the particle number density as $n \equiv \Sigma/(2m_p H)$, where m_p is the proton mass.

To determine the thermal state of the disc we assume that it is in equilibrium, i.e. we balance heating and radiative cooling ($Q_+ = Q_-$). In particular, we consider viscous heating by turbulence and spiral shocks,

$$Q_+ = \frac{9}{4}\nu\Sigma\Omega^2, \quad (5)$$

and radiative cooling

$$Q_- = 2H\Lambda, \quad (6)$$

where Λ is the cooling rate in units of $\text{erg s}^{-1} \text{ cm}^{-3}$. For the cooling process, we consider H^- free-bound emission, which is the dominant channel in the thermal evolution at $n \gtrsim 10^8 \text{ cm}^{-3}$ for a warm primordial gas in an atomic cooling halo. The form of the cooling rate is given in § 2.2.

Finally, we adopt the standard α -prescription (Shakura & Sunyaev 1973) as a model for the viscosity by gravitational torques:

$$\nu = \alpha c_s H, \quad (7)$$

where α is the viscous parameter. From hydrodynamical simulations of a self-gravitating disc, the disc is found to be susceptible to fragmentation if the viscous parameter exceeds a critical threshold value, $\alpha \gtrsim \alpha_f$ (e.g., Gammie 2001). Rice et al. (2005) have studied fragmentation conditions for various specific heat ratios, and obtained $\alpha_f \sim 0.06$. However, the critical value depends on both initial conditions and on numerical resolution (Meru & Bate

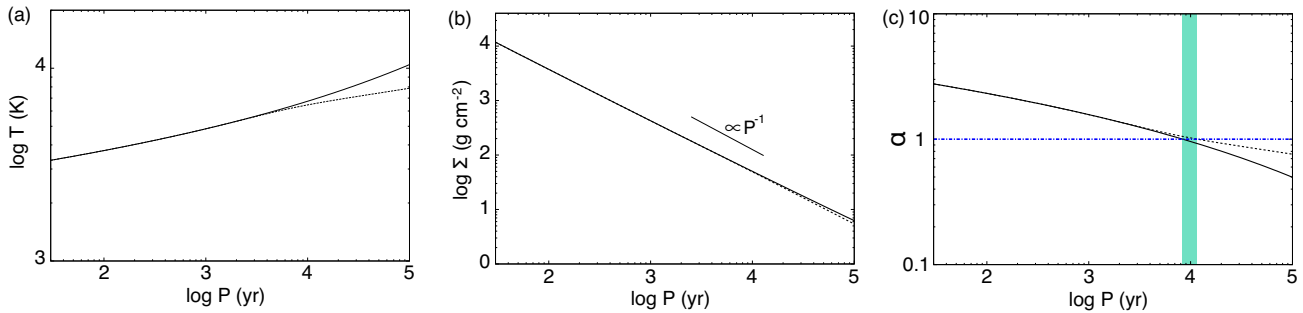


Figure 1. Radial profiles of disc quantities, shown as a function of the orbital period: (a) temperature, (b) surface density, and (c) viscous parameter. The solid curves show profiles with H^- free-bound emission as the only radiative cooling process. The dashed curves additionally include $\text{Ly}\alpha$ emission. The horizontal dot-dashed line in panel (c) indicates the critical value of the viscous parameter for fragmentation, $\alpha_f = 1$. The shaded bar marks the location of the fragmenting radius at $P_f = 2\pi/\Omega_f = 10^4$ yr (or $\Omega_f = 2 \times 10^{-11}$ s $^{-1}$).

2011a,b). Recently, Zhu et al. (2012) have considered mass loading from an infalling envelope, realistic radiative cooling, and radiative trapping of energy inside clumps, and suggested that the critical value for fragmentation is around $\alpha_f \sim 1$. Moreover, numerical simulations of fragmentation of discs with relatively high accretion rates ($\dot{M}_{\text{tot}} \sim 10^{-4} - 10^{-2} M_{\odot} \text{ yr}^{-1}$), in the context of present-day massive star formation (e.g., Krumholz et al. 2007) and Pop III star formation (Clark et al. 2011) have shown that the effective viscous parameter arising from gravitational torques is $\sim 0.1 - 1$. Based on these results, we here set $\alpha_f = 1$ as our fiducial value, and analyze disc fragmentation using the condition of $\alpha \geq \alpha_f$ following previous analytical works (e.g., Rafikov 2005; Levin 2007).

2.2 Radiative cooling and chemistry

In dense ($n \gtrsim 10^8$ cm $^{-3}$) and warm ($3000 \lesssim T \lesssim 8000$ K) primordial gas, the dominant cooling processes is the free-bound emission of H^- ions ($\text{H} + \text{e}^- \rightarrow \text{H}^- + \gamma$; Omukai 2001; Inayoshi et al. 2014). The cooling rate, in units of erg s $^{-1}$ cm $^{-3}$, is given by

$$\Lambda = \lambda(T)n^2 x_e, \quad (8)$$

where $x_e (\ll 1)$ is the free-electron fraction and $\lambda(T) \simeq 10^{-30} T$ (with T in units of Kelvin). In such a warm gas, prior to protostar formation, the electron fraction is determined by the balance between recombination ($\text{H}^+ + \text{e}^- \rightarrow \text{H} + \gamma$) and collisional ionization ($2\text{H} \rightarrow \text{H}_2^+ + \text{e}^-$). The evolution of the electron fraction follows the equation

$$\frac{dx_e}{dt} = -\alpha_{\text{rec}} n x_e^2 + \alpha_{\text{ci}} n. \quad (9)$$

At the densities of interest here, the electron fraction is in equilibrium, and given simply by

$$x_e = \sqrt{\frac{\alpha_{\text{ci}}}{\alpha_{\text{rec}}}}. \quad (10)$$

From Appendix A, we obtain the specific value of

$$\begin{aligned} x_e &\simeq f(T) n^{1/2} \exp(-\epsilon/2T) \\ &\simeq 5.0 \times 10^{-11} T^{1.2} n^{1/2} \exp(-\epsilon/2T). \end{aligned} \quad (11)$$

2.3 Radial profile of the disc

We next obtain the properties of the marginally fragmenting disc, using the energy conservation equation ($Q_+ = Q_-$). Using Eq. (2), the particle density can be written by

$$n = \frac{\Sigma \Omega}{2m_p c_s} = \frac{\Omega^2}{2m_p \pi G}. \quad (12)$$

Then, we can solve the energy conservation equation with respect to Ω :

$$\Omega^2 = \frac{3\dot{M}_{\text{tot}} (2\pi G m_p)^{5/2}}{8\pi c_s \lambda(T) f(T)} \exp(\epsilon/2T). \quad (13)$$

We present the profiles of the temperature, surface density, and viscous parameter as a function of Ω for the case of $\dot{M}_{\text{tot}} = 0.1 M_{\odot} \text{ yr}^{-1}$ in Figure 1. As described above, we assume that fragmentation occurs efficiently at the radii where $\alpha \gtrsim \alpha_f \simeq 1$. From Figure 1(c), we find that fragmentations occur in the central regions where the orbital period is shorter than 10^4 yr. Within the fragmenting region, the surface density is approximately given by $\Sigma = \Sigma_f (\Omega/\Omega_f)$, where $\Sigma_f = 50$ g cm $^{-2}$ and $\Omega_f = 2 \times 10^{-11}$ s $^{-1}$, respectively. During the earliest stages, i.e. prior to the formation of any central protostar embryo, or immediately following it, the disc mass dominates the central protostellar mass. We can then obtain the radius within which the disc fragments effectively,

$$R_f = \frac{2\pi G \Sigma_f}{\Omega_f^2} \simeq 2 \times 10^{-2} \text{ pc}. \quad (14)$$

Moreover, during this stage, the profiles of the surface density, disc mass, and number density can be written as functions of the radial distance R from the central protostar:

$$\Sigma = \Sigma_f \left(\frac{R}{R_f} \right)^{-1}, \quad (15)$$

$$M_d \simeq 430 M_{\odot} \left(\frac{R}{R_f} \right), \quad (16)$$

and

$$n \simeq 6 \times 10^8 \text{ cm}^{-3} \left(\frac{R}{R_f} \right)^{-2}, \quad (17)$$

respectively. The typical mass of the clumps formed at $\simeq R_f$

is estimated as

$$M_c \simeq \Sigma_f H_f^2 \simeq 30 M_\odot. \quad (18)$$

These disc profiles and the clump mass are in good agreement with the highest resolution results in the numerical simulations by Regan et al. (2014), lending credence to our simplified ‘toy’ model.

In the above, we have assumed that the mass of the central protostar is negligible. However, the central protostar grows via rapid accretion and having a central point source can then modify the disc structure. After $\gtrsim 10^4$ yr, the gas within R_f accretes on to the central protostar, and the protostellar mass exceeds the disc mass within R_f . The fragmentation radius (defined by $\alpha(R_f) = 1$) remains roughly constant for the first \sim a few $\times 10^4$ yr, after which it begins to move outward slowly, according to

$$R_f = \left(\frac{GM_*}{\Omega_f^2} \right)^{1/3} \quad (19)$$

$$\simeq 5 \times 10^{-2} \text{ pc} \left(\frac{M_*}{10^4 M_\odot} \right)^{1/3} \propto t^{1/3},$$

where M_* is the mass of the protostellar embryo at the center, and we have assumed that the central accretion rate remains constant over time. In the regions where $M_* > M_d$, the orbital frequency is proportional to $R^{-3/2}$ and thus the surface density and mass of the disc are given by

$$\Sigma = \frac{\Sigma_f}{\Omega_f} \sqrt{\frac{GM_*}{R^3}} \quad (20)$$

and

$$M_d = 4\pi \frac{\Sigma_f}{\Omega_f} \sqrt{GM_* R}, \quad (21)$$

respectively. The radius where $M_* = M_d$ is given by

$$R_{g*} = \frac{M_* \Omega_f^2}{16\pi^2 G \Sigma_f^2} \propto t. \quad (22)$$

The condition $R_f \lesssim R_{g*}$ is satisfied when the protostellar mass exceeds $\simeq 3 \times 10^3 M_\odot$, which corresponds to $t \simeq 3 \times 10^4$ yr $(M_*/3 \times 10^3 M_\odot)(\dot{M}_{\text{tot}}/0.1 M_\odot \text{ yr}^{-1})^{-1}$. For convenience in the following section (§ 3), we define the transition epoch as $t_{g*} = 10^5$ yr neglecting the difference of the factor of 3 because the ratio of $R_{g*}/R_f \propto t^{2/3}$ does not change significantly in the range $3 \times 10^4 < t < 10^5$ yr. Therefore, we use Eq. (15) and (16) for $t < t_{g*}$ and Eqs. (20) and (21) for $t \geq t_{g*}$ (hereafter the ‘late phase’) for the radial profile of the disc, respectively.

3 FATE OF THE CENTRAL PROTOSTAR AND CLUMPS

In the fragmenting disc, the evolution of the clumps is determined by several physical processes, including migration, accretion, and evolution to ZAMS stars. In this section, we consider these processes, and discuss the fate of the clumps formed at the fragmentation radius.

3.1 Clump migration

The clumps formed at R_f interact with the disc through gravitational torques, which results in their orbital evolution, i.e. ‘migration’. We first discuss the time-scales for

limiting cases of inward migration applicable to planets embedded in smooth discs; this serves as a useful reference. We then discuss the complications and uncertainties for protogalactic discs, arising from the fact that the disc is clumpy, and the nominal migration rate is very rapid.

Limiting cases of idealized migration are well-known in the theory of disc-planet interactions. One is the case when the planet mass is so small that the perturbation induced in the disc is in the linear regime. The density waves excited in the disc by the planet exert torques on the planet through resonances, and thus promote the migration (so-called Type I migration; e.g. Goldreich & Tremaine 1980; Ward 1986). The characteristic time-scale of Type I migration is

$$t_{\text{mig,I}} = \frac{1}{4Cq\mu} \left(\frac{H}{R} \right)^2 \frac{2\pi}{\Omega}, \quad (23)$$

where $C = 3.2 + 1.468 \xi$, ξ is the power of the surface density profile $\Sigma(R)$, $q = M_c/M_*$, and $\mu = \pi \Sigma R^2/M_*$ (Tanaka et al. 2002). A second case is when the planet mass is massive enough to clear a gap in the disc (but still less massive than the local disc). Then, the planet migrates inward on approximately the disc’s viscous time-scale (so-called Type II migration; e.g. Lin & Papaloizou 1986; Ward 1997):

$$t_{\text{mig,II}} \simeq t_{\text{vis}} = \frac{1}{3\pi\alpha} \left(\frac{R}{H} \right)^2 \frac{2\pi}{\Omega}. \quad (24)$$

The theoretical basis for these time-scales is derived from idealized setups, assuming point-like planets and a smooth disc profile. Whether these results are applicable for an extended clump, in a gravitationally unstable and lumpy disc, as we discuss in this paper is poorly known. Nevertheless, recent numerical simulations have provided some useful information. In particular, low-mass planets embedded in a turbulent disc have been found to migrate inwards, despite the stochastic kicks due to the turbulent density fluctuations, essentially on the time-scale of Type I migration (Baruteau et al. 2011; Michael et al. 2011). If the clump grows via accretion and opens a gap during its migration in the gravitationally unstable disc, a transition between Type I and Type II migration occurs and the migration speed slows down (Zhu et al. 2012).

From the disc properties discussed in § 2.3, we expect that the characteristic migration time shifts from that of Type II to that of Type I, because the mass ratio q decreases as the central protostar (and the mass of the corresponding steady-state disc) grows. We therefore estimate the transition epoch and the migration time for the late phase ($M_* \gtrsim 10^4 M_\odot$) using Eq. (23). The gap-opening condition has been investigated by many authors (e.g., Lin & Papaloizou 1979; Rafikov 2002; Crida et al. 2006; Duffell & MacFadyen 2013), but again, remains poorly known for gravitationally unstable and clumpy discs. To give a conservative estimate, we here do not discuss the gap-opening condition, but compare the time-scales of Type I and II migration. The ratio of the two time-scales at R_f (Eq. 19) is independent of the central mass, and is given by

$$\frac{t_{\text{mig,I}}}{t_{\text{mig,II}}} \simeq \frac{0.4}{q} \left(\frac{H}{R} \right)^3 \simeq 2.0 \left(\frac{M_c}{30 M_\odot} \right)^{-1}, \quad (25)$$

where we have used the condition $Q = 1$. Since the clumps grow via accretion at a typical rate of at least $\dot{M}_c \sim$ a few \times

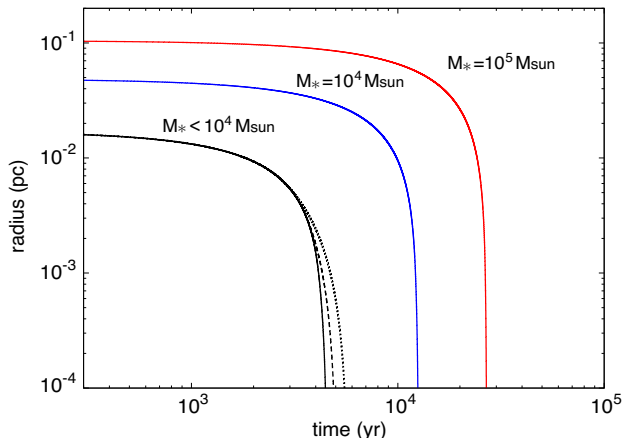


Figure 2. The decay time of the clump’s orbit, for the case of $M_* < 10^4 M_\odot$ ($M_* < M_d$; $t < t_{g*}$), $M_* = 10^4$ and $10^5 M_\odot$ ($M_* > M_d$; $t > t_{g*}$), respectively. In each case, the initial position of the clump is set to the fragmentation radius R_f . In the first ($M_* < 10^4 M_\odot$) case, we show the slow-down of the migration expected if the clump grows by accretion at a rate of $f\dot{M}_{\text{tot}}$ with $f = 0$ (solid), 0.2 (dashed), and 0.5 (dotted).

$10^{-3} M_\odot \text{ yr}^{-1}$ (see § 3.2), the clump migrates towards the central protostar on a time-scale comparable or shorter than that in the Type II case, independent of the presence or absence of a gap. In the following, we therefore adopt $t_{\text{mig,II}}$ as a conservative choice for the migration time-scale.

We first estimate the migration time for the case that the self-gravity of the disc within R_f dominates the protostellar gravity (i.e. $t < t_{g*}$). At this stage, the mass of the central protostar is $\lesssim 10^4 M_\odot$. From Eqs. (16) and (18), the clump mass is initially smaller than the local disc mass ($M_c \simeq 0.1 M_d$). In the disc-dominated case, the orbital decay time of the clump ($t_{\text{mig}} = -R/\dot{R}$) is approximately given by the viscous time (Eq. 24; see also Duffell et al. 2014 who find a factor of few faster migration in the case they studied). Since $H/R = Q/2 \simeq 0.5$ at R_f , $t_{\text{mig}} \sim 0.4(2\pi/\Omega_f) \sim 4 \times 10^3$ yr. Thus, we find that the clump orbit decays slightly faster than the orbital period. This follows essentially from our assumption of $\alpha_f = 1$, and leads to a complication: Eq. (24) for the Type II migration rate is strictly valid only for $t_{\text{mig}} > 2\pi/\Omega$ because the torques exerted on the clump are assumed to be averaged over an orbit (at a fixed radius). Despite this complication, we can still safely conclude $t_{\text{mig}} \lesssim 2\pi/\Omega$. This is because assuming a slower migration ($t_{\text{mig}} \gtrsim 2\pi/\Omega$) would justify the use of orbit-averaged Type II torques, which would then yield the contradiction $t_{\text{mig}} < 2\pi/\Omega$.

When the clump migrates to $\simeq 0.1 R_f$, its mass becomes comparable to the local disc mass (neglecting for now any growth of either the disc or the clump during the migration). Within $\sim 0.1 R_f$, the migration speed slows down because the disc outside the clump can no longer absorb the orbital angular momentum of the clump (Syer & Clarke 1995). In the clump-dominated case, the migration time is somewhat modified as

$$t_{\text{mig}} \simeq q_B^{-k} t_{\text{vis}}, \quad (26)$$

where

$$q_B = \frac{(1+q)\dot{M}_{\text{tot}}}{M_c} t_{\text{vis}} \quad (27)$$

$$\simeq 1.1 \left(\frac{1+q}{1.1} \right) \left(\frac{M_c}{30 M_\odot} \right)^{-1} \left(\frac{\dot{M}_{\text{tot}}}{0.1 M_\odot \text{ yr}^{-1}} \right) \left(\frac{t_{\text{vis}}}{300 \text{ yr}} \right)$$

and

$$k = 1 - \left(1 + \frac{\partial \ln \Sigma}{\partial \ln \dot{M}_{\text{tot}}} \right)^{-1} \simeq 0.4. \quad (28)$$

In Figure 2, we show the evolution of the orbital radius of the clump (black lines: $M_* < 10^4 M_\odot$). The horizontal axis is the time from the onset of the orbital decay at R_f . To see the effect of the slow down, we assume that the clump grows at the accretion rate of $f\dot{M}_{\text{tot}}$ with $f = 0$ (solid curve), 0.2 (dashed), and 0.5 (dotted), respectively. In each case, the clump’s orbit decays within 10^4 yr, even if we consider the slow down of the migration.

Next, we consider the case that the protostellar gravity exceeds the self-gravity of the disc within R_f (i.e. $t \geq t_{g*}$). In Figure 2, we show the corresponding orbital evolution for $M_* = 10^4$ (blue middle curve) and $10^5 M_\odot$ (red right most curve) as examples of this stage. In both the cases, we do not consider the clump growth because the initial clump mass is much smaller than the disc mass within R_f and thus the slow-down effect works after the orbit has decayed by more than two orders of magnitude. For $M_* = 10^5 M_\odot$, the fragmentation radius moves out to ~ 0.1 pc. In this case, the decay time becomes longer than the orbital period, and the clump could evolve into a normal massive star, rather than an SMS. However, this scenario is realized only by assuming that a SMS with $M_* \sim 10^5 M_\odot$ has already grown at the center of the disc.

3.2 Clump accretion and evolution

In the fragmenting disc, many clumps are formed within R_f and their orbits decay through interaction with the accretion disc. Since the typical density of the clumps is $\sim 10^9 \text{ cm}^{-3}$ (Eq. 17) and since they are optically thin to the H^- free-bound emission, tiny protostars are formed in the clumps within their free-fall time $\sim 10^3$ yr, which is an order of magnitude shorter than the orbital decay time. In this section, we simply estimate the accretion rate on to the clumps (which we assume quickly evolve to protostars), and then discuss the possibility of forming ZAMS stars from the clumps.

The accretion rate on to a point-like clump in a Keplerian disc, where we assume a rotationally supported disc (Regan et al. 2014), is estimated as

$$\dot{M}_c = \frac{3}{2} \Sigma \Omega (f_H R_H)^2, \quad (29)$$

where R_H is the Hill radius defined by $R(M_c/3M_*)^{1/3}$ and $f_H \sim O(1)$ (e.g., Goodman & Tan 2004). We have also assumed that the clump accretes gas orbiting in the nearby disc, within an impact parameter $f_H R_H$. At the fragmenta-

tion radius, the accretion rate is given by

$$\begin{aligned} \dot{M}_c|_{R_f} &= \frac{3}{2} \Sigma_f \Omega_f f_H^2 R_f^2 \left(\frac{M_c}{3M_*} \right)^{2/3} \\ &\simeq 1.1 \times 10^{-2} M_\odot \text{ yr}^{-1} \left(\frac{f_H}{1.5} \right)^2 \left(\frac{M_c}{30 M_\odot} \right)^{2/3}, \end{aligned} \quad (30)$$

which is similar to the critical rate ($\approx 4 \times 10^{-3} M_\odot \text{ yr}^{-1}$) at which the evolution of a protostar changes qualitatively (Omukai & Palla 2001, 2003). Below the critical rate, the protostar grows to a usual ZAMS star. Above the critical rate, the protostar evolves instead to a structure with a bloated envelope resembling a giant star (Hosokawa et al. 2012, 2013). The accretion rate given by Eq. (30) is only a factor of ≈ 2 above the critical value. We therefore consider the case in which some of the clumps grow at a sub-critical rate and form massive ZAMS stars.

The protostar embedded in the clump begins to undergo Kelvin-Helmholtz (KH) contraction, losing energy by radiative diffusion. After the contraction, the star reaches a ZAMS star when the central temperature increases to $\sim 10^8 \text{ K}$ and hydrogen burning begins (Omukai & Palla 2001, 2003). Below the critical rate, the time-scale of the KH contraction is estimated as

$$t_{\text{KH}} \simeq \frac{M_c}{\dot{M}_c} \gtrsim 10^4 \text{ yr} \left(\frac{M_c}{30 M_\odot} \right) \left(\frac{\dot{M}_c}{3 \times 10^{-3} M_\odot \text{ yr}^{-1}} \right)^{-1}. \quad (31)$$

Thus, it is longer than both the migration time for $M_* \leq 10^4 M_\odot$ and the orbital period at the fragmentation radius. Therefore, most clumps formed promptly in the early (disc-dominated) phase are expected to migrate and merge with the central protostar before reaching the massive ZAMS stars ($M_* \leq 10^4 M_\odot$). On the other hand, clumps formed in the late (central protostar-dominated) phase ($M_* > 10^4 M_\odot$) could survive and evolve to ZAMS stars.

3.3 Radiative feedback

As we have seen in § 3.2, the decay time of the clump orbit becomes longer than the KH time during the late stage for $M_* > 10^4 M_\odot$. In this case, the clump can contract by losing energy and reach the ZAMS star before migrating towards the central protostar. This, however, requires a central SMS to be already present. On the other hand, even during the early stage for $M_* < 10^4 M_\odot$, some clumps could survive for their KH times, because clumps interact with each other, as well as with the disc, within the fragmentation radius. In a clumpy disc, these gravitational interactions will make the orbital decay time longer or shorter stochastically, and can also cause clumps to be temporarily ejected from the disc (Escala et al. 2005; Greif et al. 2012; Zhu et al. 2012; Fiacconi et al. 2013). Some of these clumps can evolve to ZAMS stars and emit strong UV radiation, which could prevent the accretion on to the protostar and on to the disc as a whole.

We briefly estimate the number of the clumps which exist in the disc at a moment. The corresponding range where the fragmentation occurs is $\Delta R \simeq R_f$. The Hill radius of the clump at R_f is written by

$$R_H = 1.5 \times 10^{16} \text{ cm} \left(\frac{M_c}{30 M_\odot} \right)^{1/3}. \quad (32)$$

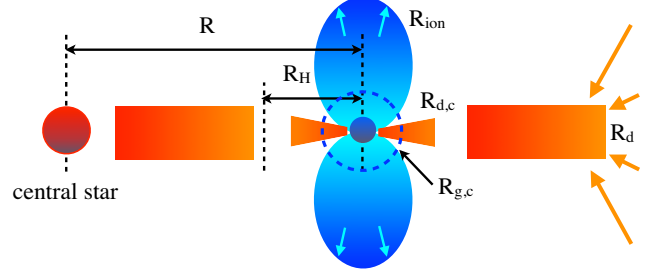


Figure 3. Schematic figure of the accretion disc and a small circum-clump disc, showing the distance of the clump from the central star R , the Hill radius of the clump R_H (Eq. 32), the size of the circum-clump disc $R_{d,c}$, the size of the HII region around the clump R_{ion} (Eq. 35), the gravitational radius of the clump $R_{g,c}$ (Eq. 36), and the size of the whole nuclear disc R_d (Eq. 39).

Thus, we roughly estimate the maximum number of the clumps which survives as

$$N_c \sim \frac{\Delta R}{R_H} \simeq 20 \left(\frac{M_*}{10^5 M_\odot} \right)^{1/3} \left(\frac{M_c}{30 M_\odot} \right)^{-1/3}. \quad (33)$$

If some clumps grow at rates higher than $\sim 10^{-3} M_\odot \text{ yr}^{-1}$ and their masses increase within t_{KH} , the maximum number decreases. We here consider $N_c \approx 10 - 20$ as a conservative value.

First, let us consider radiative feedback on the accretion on to the ZAMS star (clump) itself. Figure 3 illustrates the gas structure around the clumps and the characteristic radii. The gas accreting on to the ZAMS star makes a small circum-clump disc. The disc size is roughly estimated as $R_{d,c} \simeq R_H/3$ (Quillen & Trilling 1998), based on numerical simulations (Ayliffe & Bate 2009; Tanigawa et al. 2012). The ZAMS star emits UV radiation and an HII region is formed above and below the disc. The size of the HII region depends on the ionizing luminosity of the ZAMS star and on the density profile of the in-falling material. For simplicity, we estimate the size R_{ion} in the polar direction using Eq. (36) of McKee & Tan (2008) as

$$\frac{R_{\text{ion}}}{R_{d,c}} \simeq 0.16 \left(\frac{M_c}{30 M_\odot} \right)^{1.25} \left(\frac{\dot{M}_c}{3 \times 10^{-3} M_\odot \text{ yr}^{-1}} \right)^{-1}, \quad (34)$$

where we assume that the disc mass is equal to the clump mass and we take the temperature of the HII region to be $3 \times 10^4 \text{ K}$ (Hosokawa et al. 2011). The sound speed in the HII region is $c_{s,\text{ion}} \simeq 20 \text{ km s}^{-1}$. For a ZAMS star located at R_f , we obtain

$$R_{\text{ion}} \simeq 8.0 \times 10^{14} \text{ cm} \left(\frac{M_c}{30 M_\odot} \right)^{19/12} \left(\frac{\dot{M}_c}{3 \times 10^{-3} M_\odot \text{ yr}^{-1}} \right)^{-1}. \quad (35)$$

Since the sound-crossing time within R_{ion} is much shorter ($\sim 13 \text{ yr}$), the ionization front expands rapidly. When the front reaches the gravitational radius

$$R_{g,c} = \frac{GM_c}{c_{s,\text{ion}}^2} \simeq 1.0 \times 10^{15} \text{ cm} \left(\frac{M_c}{30 M_\odot} \right), \quad (36)$$

the ionized gas breaks out through the neutral infalling gas. The ionizing photons subsequently heat the disc surface, and thus photo-evaporation begins to suppress the accre-

tion rate. The photo-evaporation rate can be expressed as

$$\dot{M}_{\text{PE}} \simeq 3.8 \times 10^{-4} \left(\frac{\Phi_{\text{EUV}}}{10^{50} \text{ s}^{-1}} \right)^{1/2} \left(\frac{R_{\text{d,c}}}{10^{16} \text{ cm}} \right)^{1/2} M_{\odot} \text{ yr}^{-1}, \quad (37)$$

where Φ_{EUV} is the ionizing photon number flux (Tanaka et al. 2013). Using the relation $\Phi_{\text{EUV}} = 3.7 \times 10^{49} N_{\text{c}} \text{ s}^{-1} (M_{\text{c}}/60 M_{\odot})^{3/2}$ in the mass range $60 \lesssim M_{\text{c}} \lesssim 300 M_{\odot}$, we obtain

$$\dot{M}_{\text{PE}} \simeq 7.4 \times 10^{-4} \left(\frac{M_{*}}{10^5 M_{\odot}} \right)^{1/6} \left(\frac{M_{\text{c}}}{60 M_{\odot}} \right)^{3/4} M_{\odot} \text{ yr}^{-1}, \quad (38)$$

which is smaller than $\dot{M}_{\text{c}} \sim \text{a few} \times 10^{-3} M_{\odot} \text{ yr}^{-1}$ by approximately an order of magnitude. We therefore conclude that accretion on to the clump could not be suppressed by its own photoionization heating. After the H_{II} region breaks out of the disc, however, the accretion proceeds only from the shadow of the disc and thus the accretion rate is reduced. Moreover, Hosokawa et al. (2011) suggest that the gas behind the disc is shocked and accelerated outward by the pressure gradient after the expansion of the H_{II} region. This process halts the accretion at $M_{\text{c}} \approx 40 M_{\odot}$. Tanaka et al. (2013) have shown that photo-evaporation starts to suppress the accretion when $\dot{M}_{\text{PE}}/\dot{M}_{\text{c}} \gtrsim 0.2$. Note that accretion on to a clump inside R_{f} cannot be suppressed, even if the H_{II} region expands by a large factor. In particular, a clump growing at a super critical rate, $\dot{M}_{\text{c}} \gtrsim 10^{-2} M_{\odot} \text{ yr}^{-1}$, is not affected by the radiative feedback because $\dot{M}_{\text{PE}}/\dot{M}_{\text{c}} \lesssim 0.08$.

Next, we discuss the possibility that the ionizing photons from the collection of all ZAMS stars together suppress the accretion (with $\dot{M}_{\text{tot}} \simeq 0.1 M_{\odot} \text{ yr}^{-1}$) from the parent cloud on to the disc as a whole. To make our discussion conservative, we assume that the clumps which emit strong UV radiation grow at the rate just below the critical accretion rate. For $M_{*} \sim 10^5 M_{\odot}$, the orbital decay time is $\sim 3 \times 10^4 \text{ yr}$ and so each clump then grows to $\sim 100 M_{\odot}$. The corresponding total ionizing photon rate is $\sim 1.1 \times 10^{51} \text{ s}^{-1}$. From numerical simulations of the gravitational collapse of an atomic-cooling cloud (Inayoshi et al. 2014), the rotational velocity is proportional to the Keplerian velocity, $v_{\text{rot}} = f_{\text{Kep}} v_{\text{Kep}}$, with $f_{\text{Kep}} \simeq 0.5$. From this relation, the size of the whole disc around the central protostar is given by

$$R_{\text{d}} = f_{\text{Kep}}^2 R_{\text{env}}, \quad (39)$$

$$\simeq 2.5 \text{ pc} \left(\frac{f_{\text{Kep}}}{0.5} \right)^2 \left(\frac{R_{\text{env}}}{10 \text{ pc}} \right),$$

where R_{env} is the size of the quasi-spherical parent cloud fuelling the inner disc. We approximate R_{env} using a critical Bonnor-Ebert sphere with a temperature of 8,000 K and a central density of 10^4 cm^{-3} , which corresponds to that of the gravitationally unstable core in the atomic cooling haloes without H_2 molecules (e.g., Wise et al. 2008). Therefore, we obtain $\dot{M}_{\text{PE}} = 3.5 \times 10^{-2} M_{\odot} \text{ yr}^{-1} (\Phi_{\text{EUV}}/1.1 \times 10^{51} \text{ s}^{-1})^{1/2} (R_{\text{d}}/2.5 \text{ pc})^{1/2}$ and thus $\dot{M}_{\text{PE}}/\dot{M}_{\text{tot}} \simeq 0.35$, which is comparable or only slightly above the critical value. Therefore, even with conservative assumptions, the strong UV radiation cannot deplete the gas supply on to the disc from the parent cloud, and the central protostar can grow to a SMS star with $M_{*} \simeq 10^5 M_{\odot}$.

4 FRAGMENTATION BY METALS: DUST COOLING

The site envisioned for forming a SMS is atomic cooling gas in a halo with virial temperature $> 10^4 \text{ K}$, in which H_2 cooling is prohibited prior to and throughout the protostellar collapse. Recent numerical simulations suggest that the majority of the atomic cooling haloes are polluted by heavy elements due to Pop III supernovae from prior star formation (Greif et al. 2010; Wise et al. 2012). The resulting metallicity is $Z \lesssim 10^{-4} Z_{\odot}$ ($\lesssim 10^{-3} Z_{\odot}$) if the Pop III supernovae are core-collapse type (pair-instability type). If the gas is slightly polluted with $Z \gtrsim 5 \times 10^{-6} Z_{\odot}$, the temperature decreases below $\sim 500 \text{ K}$ by dust cooling (Omukai et al. 2008), which could promote efficient fragmentation. The details of this fragmentation, and whether dust cooling ultimately prevents SMS formation, are not yet understood.

The temperature of the gas with dust grains begins to decrease through heat exchange with cool dust grains ($T_{\text{gr}} \ll T$) when collisions between gas particles and dust are sufficiently frequent. Collisional cooling of the gas is efficient until $T \sim 500 \text{ K}$, where the gas and dust is thermally coupled ($T \simeq T_{\text{gr}}$). At the cooling phase, the compressional heating and collisional cooling are balanced as

$$\frac{\rho c_{\text{s}}^2}{t_{\text{ff}}} \simeq H_{\text{gr}}, \quad (40)$$

where $t_{\text{ff}} = \sqrt{3\pi/(32G\rho)}$ is the free-fall time and H_{gr} is the energy exchange rate (in $\text{erg s}^{-1} \text{ cm}^{-3}$) between the gas and dust, defined by

$$H_{\text{gr}} \simeq 2k_{\text{B}} T n_{\text{H}} n_{\text{gr}} \sigma_{\text{gr}} c_{\text{s}}, \quad (41)$$

for $T \gg T_{\text{gr}}$ (Schneider et al. 2006, 2012). We adopt the number density and cross-section of the dust particles from Semenov et al. (2003),

$$\frac{n_{\text{gr}} \sigma_{\text{gr}}}{\rho} = 4.7 \times 10^{-2} \left(\frac{Z}{10^{-4} Z_{\odot}} \right) \text{ cm}^2 \text{ g}^{-1}, \quad (42)$$

where the depletion factor of metals to dusts is assumed as high as the present-day Galactic value $f_{\text{dep}} \simeq 0.5$. From Eqs. (40), (41), and (42), we obtain

$$n \simeq 6.8 \times 10^7 \text{ cm}^{-3} \left(\frac{T}{6000 \text{ K}} \right)^{-1} \left(\frac{Z}{10^{-4} Z_{\odot}} \right)^{-2}, \quad (43)$$

above which the temperature begins to decrease compared to the zero-metallicity case. The density given by Eq. (43) is comparable to that at the fragmenting radius. This implies that the discussion in § 3 remains valid in metal-polluted gas, as long as the metallicity remains below $Z \lesssim 10^{-4} Z_{\odot}$. We conclude that disc fragmentation cannot prevent SMS formation, as long as the metallicity is below this value. On the other hand, at higher metallicity ($Z > 3 \times 10^{-4} Z_{\odot}$), the gas temperature rapidly decreases by metal-line cooling at densities below $\sim 10^4 \text{ cm}^{-3}$ (Omukai et al. 2008; Inayoshi & Omukai 2012). Numerical simulations of metal-enriched collapse into atomic cooling haloes also capture the character of gas fragmentation for $Z \gtrsim 10^{-3} Z_{\odot}$ (Safranek-Shrader et al. 2014a,b). The outcome would be a compact star-cluster which consists of many low-mass stars with $\sim 1 M_{\odot}$ (Tanaka & Omukai 2014).

5 DISCUSSION AND CONCLUSIONS

In this paper, we discussed the properties of a disc around the embryo of a SMS ($\gtrsim 10^5 M_\odot$), expected to be present in a primordial gas without H_2 molecules in massive haloes with virial temperature $\gtrsim 10^4$ K. A high accretion rate $\gtrsim 0.1 M_\odot \text{ yr}^{-1}$, sustained for $\gtrsim 10^5 \text{ yr}$, is required to form a SMS. The inner region of such a disc is gravitationally unstable, and fragments into $O(10)$ clumps with characteristic mass of $\sim 30 M_\odot$. We discuss the possibility that this fragmentation prevents SMS formation. We argue that most of the clumps formed in the disc rapidly migrate towards the central protostar and merge with it. The orbital decay time is shorter than or comparable to the orbital period of the clumps ($\lesssim 10^4 \text{ yr}$). Some of the clumps can grow via accretion and evolve to ZAMS stars within their KH time, either because they survive longer due to the stochasticity of the migration process, or because they form later, further out in the disc.

Our toy model, on which these conclusions are based, can be tested against simulations of Pop III star formation in lower mass minihaloes. In this case, the dominant cooling process is H_2 line emission ($T \sim 10^3$ K) and the resulting accretion rate is $\sim 10^{-3} - 10^{-2} M_\odot \text{ yr}^{-1}$, which is smaller than that in the SMS formation case. According to high-resolution numerical simulations by Greif et al. (2012), clump formation occurs at ~ 10 AU ($\Sigma \sim 5 \times 10^3 \text{ g cm}^{-2}$, $\Omega \sim 0.1 \text{ yr}^{-1}$, $c_s \sim 2.5 \text{ km s}^{-1}$ and $M_d \sim 1 M_\odot$ in their Fig. 2) in the gravitationally unstable disc at the early stage $\lesssim 10 \text{ yr}$. From Eq. (14), we can estimate the fragmentation radius as ~ 20 AU, which is consistent with the fragmentation radii in the simulations. At this stage, the average accretion rate is high, $\dot{M}_{\text{tot}} \simeq 10^{-2} M_\odot \text{ yr}^{-1}$ in their Fig. 8. From Eq. (3), (4), (7), and $Q \simeq 1$,

$$\dot{M}_{\text{tot}} \simeq 3\alpha \frac{c_s^3}{G}. \quad (44)$$

Using these equations, the sound speed at the fragmentation radius ($\alpha_f = 1$) is estimated as $c_s = 2.5 \text{ km s}^{-1}$, which agrees well with the numerical result. The viscous time at ~ 10 AU is roughly estimated as $t_{\text{vis}} \sim M_d / \dot{M}_{\text{tot}} \sim 10^2 \text{ yr}$. Since some clumps migrate inward within 10 yr ($< t_{\text{vis}}$) in simulation, other effects (Type I migration and interaction between clumps) could accelerate the clumps migration. Therefore, our results from the toy model are expected to be conservative, and appear to capture the essential features of disc fragmentation and clump migration.

The gas in most of the massive haloes is likely to be polluted by heavy elements due to prior star formation and Pop III supernovae. With the metallicity of $5 \times 10^{-6} \lesssim Z \lesssim 10^{-4} Z_\odot$, the dust cooling decreases the temperature rapidly and could promote the fragmentation at $n > 10^8 \text{ cm}^{-3}$ (Omukai et al. 2008). As a result, the existence of dusts has been considered as one of the most severe obstacles to the SMS formation. However, the fragmentation induced by the dust cooling is expected to occur only within the fragmenting radius we estimated. This means that the clumps formed by the dust cooling can migrate towards the center on a time-scale comparable to the orbital period, in the same way as the primordial case. We conclude that the SMS formation is not prevented, unless the metal-line cooling dominates for $Z \gtrsim 3 \times 10^{-4} Z_\odot$. Our results therefore remove a significant obstacle for SMS formation.

Our estimates for the orbital decay time of the clumps are based on the well-known formulae of Type I and II planetary migration. Although some numerical simulations find that these formulae remain approximately valid in gravitationally unstable and clumpy discs, there are many uncertainties regarding the migration rate in this case. For example, we neglect the orbital eccentricities of the clumps. The clumps formed by the disc fragmentation are expected to have eccentric orbits and thus the angular momentum transfer between the disc and clumps could change from the case of the circular orbits. Moreover, in such a situation, the interaction with eccentric clumps retard the orbital decay of the other clumps (Fiacconi et al. 2013). To estimate the migration time within the clumpy disc around the SMS star, more sophisticated numerical simulations are necessary.

It is worth further emphasizing the limitations and uncertainties of our disc model. In Figure 1, we present the disc profile based on cooling by free-bound emission of H^- and thermal equilibrium. Hydrogen atomic cooling ($\text{Ly}\alpha$ and two-photon emission) dominates at $T \gtrsim 8000$ K ($P > 10^4 \text{ yr}$). To quantify the effect, we include $\text{Ly}\alpha$ cooling ($\Lambda = \lambda_{\text{Ly}\alpha} n^2 x_e$; Glover & Jappsen 2007) in the limiting optically thin case (dashed lines in Fig. 1). Since the gas is in fact optically thick to the $\text{Ly}\alpha$ photons at $n > 10^5 \text{ cm}^{-3}$, and the cooling efficiency of the two-photon channel is smaller than the $\text{Ly}\alpha$ emission, the dashed lines overestimate the additional atomic cooling rate. Nevertheless, the profiles deviate from our fiducial disc model only modestly, beginning at $P > 10^4 \text{ yr}$ and thus the critical period changes at most within the shaded region in Figure 1 (c).

The crucial ingredient of this paper is the critical value of the effective viscous parameter α_f for fragmentation. In our model, the fragmentation radius depends sensitively on the value of α_f . For example, if we chose $\alpha_f = 0.5$, we obtain $\Omega_f = 2 \times 10^{-12} \text{ s}^{-1}$ ($P = 10^5 \text{ yr}$), $\Sigma_f = 6 \text{ g cm}^{-2}$, $M_c \simeq 400 M_\odot$ and $R_f \simeq 0.2 \text{ pc}$. In this case, the orbital decay time becomes longer than the KH time of the clumps by a factor of 4, and most of the clumps may evolve to massive stars and emit strong UV radiation. Nevertheless, the number of clumps decreases by a factor of 2 from the case of $\alpha_f = 1.0$ (see Eq. 33). Therefore, we expect that our main conclusion also does not change. However, if $\alpha_f \lesssim 0.1$, the fragmenting radius moves outside the size of the whole disc given by Eq. (39), which means that the disc cannot exist, i.e., our model is no longer self-consistent. To explore the precise value of α_f is left for future investigations. In particular, our results motivate high-resolution numerical simulations similar to Regan et al. (2014). Moreover, more realistic treatments of radiative cooling and chemical reactions at densities higher than $\sim 10^8 \text{ cm}^{-3}$ (Inayoshi et al. 2014) should be included since the fragmentation efficiency strongly depends on the equation of state of the gas.

Despite these caveats, we expect that SMS formation in metal-poor gas in atomic-cooling haloes is difficult to avoid, as it requires that the high mass inflow rate, $\gtrsim 0.1 M_\odot \text{ yr}^{-1}$, is democratically distributed among $O(100)$ fragments (so that *none* of them accretes at a super critical rate for SMS formation) and that most of these fragments survive rapid migration and avoid coalescence with the growing central protostar for several orbital times. The toy models presented in this paper disfavor this scenario.

ACKNOWLEDGEMENTS

We thank Greg Bryan, Kazuyuki Omukai, Takashi Hosokawa, Kei Tanaka and Eli Visbal for fruitful discussions. This work is supported by the Grants-in-Aid by the Ministry of Education, Culture, and Science of Japan (KI), and by NASA grant NNX11AE05G (ZH).

APPENDIX A: IONIZATION DEGREE

In this appendix, we briefly describe how to obtain the expression of Eq. (11). The reaction rate coefficient of radiative recombination α_{rec} is a function of temperature (Ferland et al. 1992). On the other hand, that of the collisional ionization α_{ci} has a complex form (Omukai 2001)

$$\alpha_{\text{ci}} = \alpha_{\text{inv}} \left(\frac{z_{\text{H}_2^+} z_{\text{e}}}{z_{\text{H}}^2} \right) 3.6034 \times 10^{-5} \exp(-\epsilon/T), \quad (\text{A1})$$

and

$$\alpha_{\text{inv}} = 1.32 \times 10^{-6} T^{-0.76} f_{1\text{st,ex}}, \quad (\text{A2})$$

where $z_{\text{H}(\text{H}_2^+, \text{e})}$ are the partition functions, $\epsilon = 1.2713 \times 10^5$ K, and $f_{1\text{st,ex}}$ is defined by

$$f_{1\text{st,ex}} = \frac{n}{n + n_{\text{H,cr}}}, \quad (\text{A3})$$

and

$$\frac{n}{n_{\text{H,cr}}} = \frac{C_{21}}{A_{21}\beta_{21} + A_{2\text{ph}}} = \frac{\gamma_{\text{H},21}x_{\text{H}} + \gamma_{\text{e},21}x_{\text{e}}}{A_{21}\beta_{21} + A_{2\text{ph}}}n, \quad (\text{A4})$$

where C_{21} is the collisional transition rate, A_{21} ($A_{2\text{ph}}$) the radiative transit rate from the first excited state to the ground state (two-photon emission, respectively), and β_{21} the escape probability of photons with 10.2 eV (see Omukai 2001 in details). For a wide range of densities ($10^6 < n < 10^{14} \text{ cm}^{-3}$), the following approximation is valid:

$$\begin{aligned} f_{1\text{st,ex}} &\approx \frac{n}{n_{\text{H,cr}}} \approx \frac{\gamma_{\text{H},21}x_{\text{H}}}{A_{2\text{ph}}}n \\ &\approx 4.3 \times 10^{-16} n T^{0.57} \quad (500 < T < 10^4 \text{ K}). \end{aligned} \quad (\text{A5})$$

REFERENCES

- Agarwal, B., Khochfar, S., Johnson, J. L., et al. 2012, MNRAS, 425, 2854
- Alvarez, M. A., Wise, J. H., & Abel, T. 2009, ApJL, 701, L133
- Ayliffe, B. A., & Bate, M. R. 2009, MNRAS, 397, 657
- Baruteau, C., Meru, F., & Paardekooper, S.-J. 2011, MNRAS, 416, 1971
- Begelman, M. C., Volonteri, M., & Rees, M. J. 2006, MNRAS, 370, 289
- Bromm, V., & Loeb, A. 2003, ApJ, 596, 34
- Ceverino, D., Dekel, A., & Bournaud, F. 2010, MNRAS, 404, 2151
- Clark, P. C., Glover, S. C. O., Smith, R. J., et al. 2011, Science, 331, 1040
- Crida, A., Morbidelli, A., & Masset, F. 2006, Icarus, 181, 587
- Dijkstra, M., Haiman, Z., Mesinger, A., & Wyithe, J. S. B. 2008, MNRAS, 391, 1961
- Dijkstra, M., Ferrara, A., & Mesinger, A. 2014, MNRAS, 442, 2036
- Di Matteo, T., Khandai, N., DeGraf, C., et al. 2012, ApJL, 745, L29
- Duffell, P. C., & MacFadyen, A. I. 2013, ApJ, 769, 41
- Duffell, P. C., Haiman, Z., MacFadyen, A. I., D’Orazio, D. J., & Farris, B. D. 2014, ApJL, 792, L10
- Escala, A., Larson, R. B., Coppi, P. S., & Mardones, D. 2005, ApJ, 630, 152
- Escala, A. 2007, ApJ, 671, 1264
- Fan, X. 2006, Nature, 50, 665
- Fiacconi, D., Mayer, L., Roškar, R., & Colpi, M. 2013, ApJL, 777, L14
- Ferland, G. J., Peterson, B. M., Horne, K., Welsh, W. F., & Nahar, S. N. 1992, ApJ, 387, 95
- Fernandez, R., Bryan, G. L., Haiman, Z., & Li, M. 2014, MNRAS, 439, 3798
- Gammie, C. F. 2001, ApJ, 553, 174
- Goldreich, P., & Tremaine, S. 1980, ApJ, 241, 425
- Goodman, J., & Tan, J. C. 2004, ApJ, 608, 108
- Greif, T. H., Glover, S. C. O., Bromm, V., & Klessen, R. S. 2010, ApJ, 716, 510
- Greif, T. H., Springel, V., White, S. D. M., Glover, S. C. O., Clark, P. C., Smith, R. J., Klessen, R. S., & Bromm, V. 2011, ApJ, 737, 75
- Greif, T. H., Bromm, V., Clark, P. C., et al. 2012, MNRAS, 424, 399
- Glover, S. C. O., & Jappsen, A.-K. 2007, ApJ, 666, 1
- Haiman, Z., & Loeb, A. 2001, ApJ, 552, 459
- Hosokawa, T., Omukai, K., Yoshida, N., & Yorke, H. W. 2011, Science, 334, 1250
- Hosokawa, T., Omukai, K., & Yorke, H. W. 2012, ApJ, 756, 93
- Hosokawa, T., Yorke, H. W., Inayoshi, K., Omukai, K., & Yoshida, N. 2013, ApJ, 778, 178
- Inayoshi, K., & Omukai, K. 2011, MNRAS, 416, 2748
- Inayoshi, K., & Omukai, K. 2012, MNRAS, 422, 2539
- Inayoshi, K., Omukai, K., & Tasker, E. J. 2014, MNRAS, submitted (arXiv:1404.4630)
- Johnson, J. L., & Bromm, V. 2007, MNRAS, 374, 1557
- Johnson, J. L., Dalla Vecchia, C., & Khochfar, S. 2013, MNRAS, 428, 1857
- Krumholz, M. R., Klein, R. I., & McKee, C. F. 2007, ApJ, 656, 959
- Latif, M. A., Schleicher, D. R. G., Schmidt, W., & Niemeyer, J. 2013, MNRAS, 433, 1607
- Levin, Y. 2007, MNRAS, 374, 515
- Li, Y., Hernquist, L., Robertson, B., et al. 2007, ApJ, 665, 187
- Lin, D. N. C., & Papaloizou, J. 1979, MNRAS, 186, 799
- Lin, D. N. C., & Papaloizou, J. 1986, ApJ, 309, 846
- Lodato, G., & Natarajan, P. 2006, MNRAS, 371, 1813
- Loeb, A., & Rasio, F. A. 1994, ApJ, 432, 52
- McKee, C. F., & Tan, J. C. 2008, ApJ, 681, 771
- Meru, F., & Bate, M. R. 2011a, MNRAS, 410, 559
- Meru, F., & Bate, M. R. 2011b, MNRAS, 411, L1
- Michael, S., Durisen, R. H., & Boley, A. C. 2011, ApJL, 737, L42
- Milosavljević, M., Couch, S. M., & Bromm, V. 2009, ApJL, 696, L146
- Mortlock, D. J., Warren, S. J., Venemans, B. P., et al. 2011, Nature, 474, 616
- Omukai, K. 2001, ApJ, 546, 635
- Omukai, K., & Palla, F. 2001, ApJL, 561, L55
- Omukai, K., & Palla, F. 2003, ApJ, 589, 677
- Omukai, K., Schneider, R., & Haiman, Z. 2008, ApJ, 686, 801
- Park, K., & Ricotti, M. 2012, ApJ, 747, 9
- Quillen, A. C., & Trilling, D. E. 1998, ApJ, 508, 707
- Rafikov, R. R. 2002, ApJ, 572, 566
- Rafikov, R. R. 2005, ApJL, 621, L69
- Regan, J. A., & Haehnelt, M. G. 2009, MNRAS, 396, 343
- Regan, J. A., Johansson, P. H., & Haehnelt, M. G. 2014, MNRAS, 439, 1160
- Reisswig, C., Ott, C. D., Abdikamalov, E., et al. 2013, Physical Review Letters, 111, 151101

- Rice, W. K. M., Lodato, G., & Armitage, P. J. 2005, MNRAS, 364, L56
- Safrank-Shrader, C., Milosavljević, M., & Bromm, V. 2014, MNRAS, 438, 1669
- Safrank-Shrader, C., Milosavljević, M., & Bromm, V. 2014, MNRAS, 440, L76
- Schneider, R., Omukai, K., Inoue, A. K., & Ferrara, A. 2006, MNRAS, 369, 1437
- Schneider, R., Omukai, K., Bianchi, S., & Valiante, R. 2012, MNRAS, 419, 1566
- Semenov, D., Henning, T., Helling, C., Ilgner, M., & Sedlmayr, E. 2003, A&A, 410, 611
- Shakura, N. I., & Sunyaev, R. A. 1973, A&A, 24, 337
- Shang, C., Bryan, G. L., & Haiman, Z. 2010, MNRAS, 402, 1249
- Shapiro, S. L., & Teukolsky, S. A. 1983, *Black Holes, White Dwarfs, and Neutron Stars: The Physics of Compact Objects*. Wiley-Interscience, New York
- Shibata, M., & Shapiro, S. L. 2002, ApJL, 572, L39
- Shu, F. H. 1977, ApJ, 214, 488
- Stahler, S. W., Palla, F., & Salpeter, E. E. 1986, ApJ, 302, 590
- Stacy, A., Greif, T. H., & Bromm, V. 2010, MNRAS, 403, 45
- Syer, D., & Clarke, C. J. 1995, MNRAS, 277, 758
- Tanaka, H., Takeuchi, T., & Ward, W. R. 2002, ApJ, 565, 1257
- Tanaka, T., & Haiman, Z. 2009, ApJ, 696, 1798
- Tanaka, T., Perna, R., & Haiman, Z. 2012, MNRAS, 425, 2974
- Tanaka, K. E. I., Nakamoto, T., & Omukai, K. 2013, ApJ, 773, 155
- Tanaka, K. E. I., & Omukai, K. 2014, MNRAS, 439, 1884
- Tanigawa, T., Ohtsuki, K., & Machida, M. N. 2012, ApJ, 747, 47
- Toomre, A. 1964, ApJ, 139, 1217
- Volonteri, M., Haardt, F., & Madau, P. 2003, ApJ, 582, 559
- Vorobyov, E. I., & Basu, S. 2005, ApJL, 633, L137
- Vorobyov, E. I., & Basu, S. 2006, ApJ, 650, 956
- Ward, W. R. 1986, *Icarus*, 67, 164
- Ward, W. R. 1997, *Icarus*, 126, 261
- Willott, C. J., Delorme, P., Omont, A., et al. 2007, AJ, 134, 2435
- Wise, J. H., Turk, M. J., & Abel, T. 2008, ApJ, 682, 745
- Wise, J. H., Turk, M. J., Norman, M. L., & Abel, T. 2012, ApJ, 745, 50
- Wolcott-Green, J., Haiman, Z., & Bryan, G. L. 2011, MNRAS, 418, 838
- Zeldovich, Y. B., & Novikov, I. D. 1971, *Relativistic Astrophysics, Vol. 1, Stars and Relativity*. University of Chicago Press, Chicago
- Zhu, Z., Hartmann, L., Nelson, R. P., & Gammie, C. F. 2012, ApJ, 746, 110